

System Simulations of Complex Electrokinetic Passive Micromixers

Y. Wang, Q. Lin, T. Mukherjee

Carnegie Mellon University, Pittsburgh, PA, USA, yiw@andrew.cmu.edu

ABSTRACT

This paper presents a composable system simulation framework for complex electrokinetic passive micromixers, using an analog hardware description language integrating analytical mixer models that describe not only the behavior of individual elements, but also the interactions among them. DC schematic analysis has been performed in the framework to capture the influence of mixer topology, element dimensions, material properties and operational parameters (e.g., electric field) on the mixing performance. Accuracy (relative error < 5%) and tremendous speedup (100–10,000×) of the composable system simulations are verified by comparison to experiment and numerical data.

Keywords: mixing, system simulation, electrokinetic, micromixer, lab on a chip

1 INTRODUCTION

Micromixers are important components in Lab-on-a-Chip (LoC) systems. Efficient mixing reduces analysis time, minimizes chip-area and improves process control. Presently, a majority of LoCs use passive mixers that rely on molecular diffusion. In addition to their relatively simple fabrication processes, electrokinetic (EK) passive mixers are amenable to integration with electrophoretic analysis and ease of control. However, their efficient simulations and designs at the system-level continue to be a challenge and have not been extensively studied. Modeling methods based on electric analogy (i.e., resistor-based models) [1] assume complete mixing and may lead to extremely long channels and bulky system. Thus, the model is not suitable for system-oriented simulations and designs. Schönfeld *et al.* [2] also derived a formula that accounts for arbitrary sample concentration distributions at channel inlets. However, the formula is limited to symmetric flow ratios (i.e., the flow rates of buffer streams carrying different samples are the same), and is not applicable to modeling mixers involving general topologies and element sizes.

To address these issues, this paper presents a composable system simulation framework using an analog hardware description language (Verilog-A) integrating analytical models [3] for basic constituent mixing elements, which are capable of capturing both the behavior of the individual elements and the electric and fluidic interactions among them. The simulations illustrate the effects of mixer topology, element dimensions and sample properties on the mixing performance. Thus, it is generally applicable to the

system-level simulations and designs of practical complex EK micromixers.

2 COMPOSABLE SYSTEM SIMULATION

Our composable simulation framework consists of a model library and a simulation engine. A Verilog-A library including parameterized behavioral models for commonly used mixing elements has been developed. Users can quickly compose a complex design schematic by wiring these blocks in a reliable and efficient top-down iterative approach. Furthermore, this framework can be integrated with our other composable subsystem models [4] to achieve the system-level simulations of multi-functional LoCs. Figure 1 illustrates a practical EK serial mixing network [1] and its schematic. The system is decomposed into a set of elements including reservoirs, channels, converging and diverging intersections, which are then linked via interface parameters among adjacent elements according to the topology and physics. Cadence's integrated circuit design tool is used for schematic entry and netlisting the system topology from the schematic editor into a text file readable by the simulator (Spectre [5]) as in Ref. [4] (Similar tools from other vendors, or custom schematic entry tools and solvers that can handle both signal flow and Kirchhoffian networks could have been also used.).

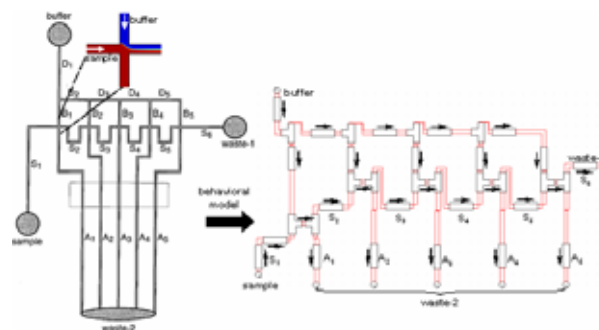


Figure 1. A complex EK serial mixing network [1] and its schematic with the hardware description behavioral models.

2.1 Interface Parameters

The first step in creating the system-level schematic for a mixer is to identify the parameters (interface parameters) that will be communicated among adjacent elements. There are two kinds of interface parameters involved in the network. One is the nodal voltage globally determined by Ohm's and Kirchhoff's laws. The other pertaining to the

sample diffusion are concentration coefficients (d_n), the Fourier series coefficients of the widthwise concentration profile and used to characterize the mixing performance. Concentration coefficients are calculated in terms of directional signal flow. That is, their values at an element outlet are determined from the values at the inlet and the element's own contribution, starting from the most upstream sample reservoirs. The schematic simulation then assigns the values at the outlet to those at the inlet of the next downstream element.

2.2 Behavioral Models

The next step is to select the list of the composable elements and develop behavioral models for each. Our behavioral model library consists of nine element models, which include reservoirs (sample and waste), straight tapered mixing channels, turns (90° or 180°, clockwise or counter-clockwise), converging and diverging intersections. The goal of each behavioral model is to capture the input-output (signal flow) relationship between the concentration coefficients and electrical resistance of each element to relate the EK current flow through the element to the inlet and outlet voltages (see Figure 2). In a simulation scheme, the steady nodal voltages at element terminals and the electric field (E) within each element will be calculated by the simulator first, given user-input voltages at all reservoirs. Then, the input-output functions of the concentration coefficients are determined.

Electrically, the straight tapered mixing channel is modeled as a resistor and the resistance is given by

$$R = \int_0^L \frac{dz}{w(z)h(z)\sigma} \quad (1)$$

where w and h are the channel width and depth (functions of the axial coordinate z), σ is the electric conductivity of the buffer solution in the channel. The concentration coefficients $d_n^{(in)}$ and $d_n^{(out)}$ at the inlet and outlet of the channel are related by [6]

$$d_n^{(out)} = d_n^{(in)} e^{-\gamma n^2 \pi^2 \tau} \quad (2)$$

where $\tau = LD/(\mu_{ek} E_{in} w_{in}^2)$, L is the channel length, w_{in} and E_{in} are the channel width and electric field at the channel inlet, D and μ_{ek} is the sample diffusivity and EK mobility respectively, γ is a factor describing the effect of the cross-sectional shape on mixing [6].

Figure 2 shows the structure of the behavioral model for the converging intersection. It has two inlets and one outlet, and acts as a combiner to align and compress upstream sample streams of an arbitrary flow ratio s (defined below) and concentration profiles side-by-side at its outlet. As its flow path lengths are negligibly small compared with those of mixing channels, converging intersection can be electrically modeled as three resistors with zero resistances between each terminal and the internal node N ,

$$R_l = R_r = R_{out} = 0 \quad (3)$$

where N corresponds to the intersection of the flow paths, and subscripts l , r and out represent the left and right inlets, and the outlet, respectively. Arrows at pins indicate the direction of the signal flow for computing concentration coefficients. Denote $d_m^{(l)}$ and $d_m^{(r)}$ the Fourier coefficients of sample concentration profiles at the left and right inlets respectively, then the coefficients $d_n^{(out)}$ at the outlet are found to be:

$$\left\{ \begin{aligned} d_0^{(out)} &= d_0^{(l)} s + d_0^{(r)} (1-s) \\ d_{n>0}^{(out)} &= s \sum_{m=0}^{m \neq ns} d_m^{(l)} \frac{f_1 \sin(f_2) + f_2 \sin(f_1)}{f_1 f_2} \\ &+ s \sum_{m=0}^{m=ns} d_m^{(l)} + (1-s) \sum_{m=0}^{m=n(1-s)} (-1)^{n-m} d_m^{(r)} \\ &+ 2(-1)^n (1-s) \sum_{m=0}^{m \neq n(1-s)} d_m^{(r)} \left(\frac{\cos(F_2/2) \sin(F_1/2)}{F_1} \right. \\ &\left. + \frac{\cos(F_1/2) \sin(F_2/2)}{F_2} \right) \end{aligned} \right. \quad (4)$$

where $s = I_l/(I_l + I_r)$ represents the interface position between incoming streams. I_l and I_r are electric currents carried by the left and right incoming buffer streams. $f_1 = (m - ns)\pi$, $f_2 = (m + ns)\pi$, $F_1 = (m + n - ns)\pi$ and $F_2 = (m - n + ns)\pi$.

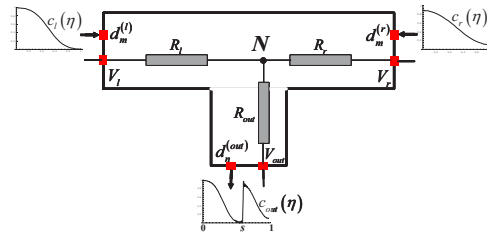


Figure 2. Structure of the behavioral model for the converging intersection.

A diverging intersection has one input and two output streams, and is the dual of the converging intersection. It splits the incoming concentration profile and electric current into two parts exiting outlets, which however can be modeled in a similar fashion as the converging intersection and the detailed solution is given elsewhere [6].

3 RESULTS AND DISCUSSION

Our composable system simulation results are shown in Figures 3-6 and Table 1. In Figure 3, multi-stream micromixers with or without focusing [7, 8] driven by EK flow is schematically represented, simulated and compared with numerical data. These kinds of micromixers improve mixing by replacing the broad sample streams (such as T-mixer) with alternating thinner streams to greatly reduce sample diffusion distance. Depending on the geometry of mixing channels, they can be further divided into those with

(Figure 3A) or without (Figure 3C) focusing. In the composable schematic, samples *a* (red) and *b* (blue) from two reservoirs are branched by successive diverging intersections into multiple streams, which are then arranged to alternate in sample content using feed channels and converging intersections connected in cascade. An interdigital concentration profile is obtained at the inlet of the mixing channel, in which the streams are mixed. Figure 4 compares concentration profiles of sample *a* obtained from schematic and numerical simulation results for both mixers at $z=L_f=L/4$ and $z=L$, where L_f and L are the lengths of the focusing and the entire mixing channels. Excellent agreement with the worst relative error of 3% is found for the focusing case. Multiple lamination of the sample is clearly seen, and the mixer with focusing facilitates sample diffusion and leads to a highly homogeneous concentration profile.

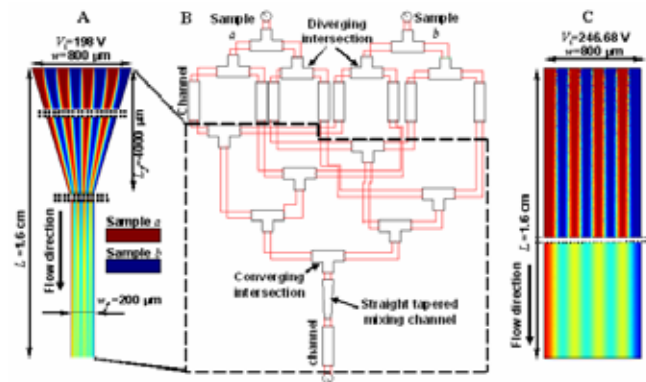


Figure 3. A focusing multi-stream micromixer (A) and its schematic (B) along with the analog hardware description behavioral models. The element of the straight tapered mixing channel can be removed to obtain the schematic for the mixer without focusing (C).

To gain the insight of the influence of the focusing and channel length on the mixing performance, an index of mixing residual, $Q = \int_0^1 |c(\eta) - c_{avg}| d\eta$, is introduced in Figure 5 to characterize the non-uniformity of the concentration profile, where c and c_{avg} are the normalized concentration profile and width-averaged concentration at the detection spot. We can see that Q drops much faster in the mixing channel with focusing than in the one without focusing, as reduced sample diffusion distance improves mixing efficiency. At $z=L_f=L/4$, a low mixing residual ($Q=0.067$) is already achieved for the mixer with focusing. From $z=L/4$ to $z=L$, a modest decrease in Q (from 0.067 to 0.048) is obtained but accounts for about 75% of the total channel length. This implies the inappropriateness of neglecting the appreciable mixing contribution made by the focusing channel [7, 8]. In addition, this indicates that shorter channel lengths with less complete, yet still sufficient mixing, may be more cost effective for some applications, demonstrating the utility of our model in the optimal choice of mixing channel lengths in mixer designs.

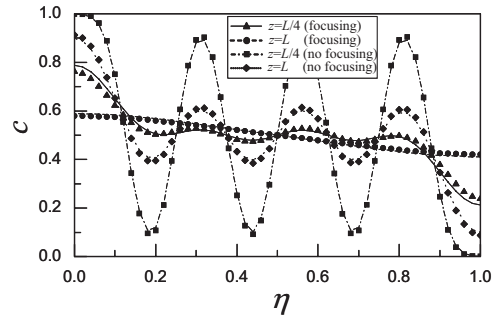


Figure 4. Comparison of numerical data (symbols) with schematic simulation results (lines) on sample *a* concentration profiles along the normalized channel width η for multi-stream micromixers with or without focusing (extracted at axial positions $L/4$ and L). $D=1 \times 10^{-10}$ m²/s, $\mu_{ek}=6 \times 10^{-8}$ m/(Vs).

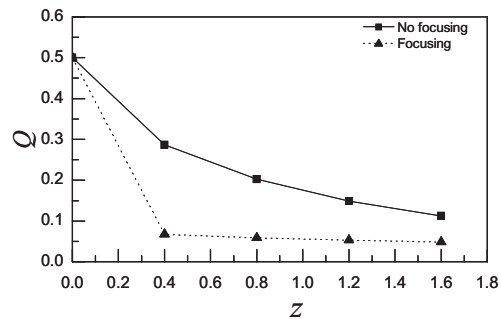


Figure 5. Schematic simulation results on the variation of the mixing residual Q along the channel length (data points are connected by lines to guide the eye) for the EK multi-stream micromixers.

Our parameterized and reusable behavioral models are well suited to study complex mixing networks [1]. Table 1 shows the comparison of schematic simulation results with experimental and numerical data on sample (rhodamine B) concentrations in the serial mixing network (Figure 1). Within the cross intersection in the network, a portion of the input sample is shunted to channels A_1 – A_5 and the rest continues along the flow direction. Repeating this unit cell generates an array of continuously diluted sample concentration in channels A_1 – A_5 that can be used for parallel bio-chemical analysis. Both complete and partial mixing cases are analyzed. When a voltage of 0.4 kV is applied to sample and buffer reservoirs with waste reservoirs grounded, sample mixing in channels S_2 – S_5 is width-wisely complete. Excellent agreement between schematic simulation and experimental results is found with an average error less than 6%. In addition to the complete mixing, the partial mixing case is also schematically simulated. A voltage of 1.6 kV, as used in the experiment in the literature [1], is applied at the sample and buffer reservoirs with the waste grounded, which increases the EK velocity and then decreases the residence time of the sample by four folds in channels S_2 – S_5 . Thereby, the

mixing in channels S_2 – S_5 is incomplete, and sample amount shunted to channels A_1 – A_5 depends on not only the electric currents in the network but also the sample concentration profiles at the exits of channels S_2 – S_5 . Results from our schematic simulations are compared with numerical data in Table 1 (a comparison to experimental data is not allowed due to a lack of knowledge of sample properties. Hence a diffusivity of $D=3\times 10^{-10}$ m²/s and an EK mobility of $\mu_{ek}=2.0\times 10^{-8}$ m²/Vs are assumed in numerical simulations). Good agreement can be obtained with an average error of 4%. At the cross-intersection following channel S_2 , the amount of sample shunted to A_2 is more than that predicted by the complete-mixing case; consequently, concentrations in channels A_3 – A_5 show the lower values, which agrees with experimental observations [1]. Netlisting and schematic simulation of this example takes about 20 seconds on a multi-user, 2-CPU 1-GHz Sun Fire 280 processors with 4 GB RAM for the first time simulation, and less than a second for subsequent iterations, leading to a 1000–20,000× speedup.

channel	Serial Mixing Network				Parallel Mixing Network		
	Complete Mixing		Partial Mixing		Complete Mixing		
	<i>c</i> (sys)	<i>c</i> (exp)	<i>c</i> (sys)	<i>c</i> (num)	channel	<i>c</i> (sys)	<i>c</i> (exp)
A_1	1	1	1	1	A_1	0	0
A_2	0.37	0.36	0.48	0.51	A_2	0.83	0.84
A_3	0.22	0.21	0.187	0.188	A_3	0.68	0.67
A_4	0.125	0.13	0.081	0.083	A_4	0.52	0.51
A_5	0.052	0.059	0.029	0.0318	A_5	0.35	0.36
					A_6	0.17	0.19
					A_7	1	1

Table 1. Comparison of system simulation results (sys) with numerical (num) and experimental (exp) data on sample concentrations in analysis channels of serial and parallel mixing networks

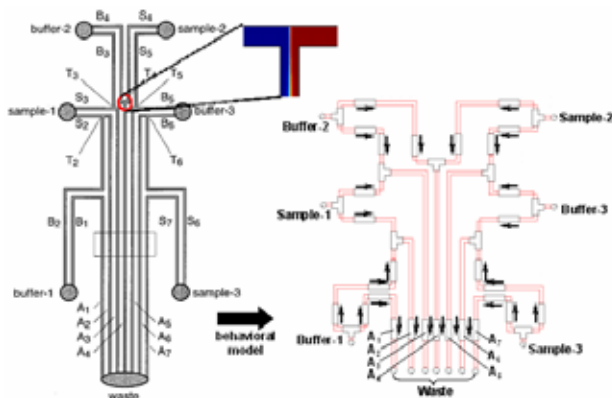


Figure 6. An EK parallel mixing network [1] and its schematic with the hardware description behavioral models.

Parallel mixing networks [1] can be represented and simulated in a similar fashion. In such a network, all the channels are designed with the similar cross-sectional area. Thus, at the T-intersection (T_2 – T_6) the currents from the sample and buffer reservoirs are inversely proportional to the lengths (Ohm’s law) of their feed channels (B_1 – B_6 and S_2 – S_7), given a single constant voltage (1 kV) applied to all sample and buffer reservoirs. Therefore, through proper choice of the lengths of those feed channels, an array of

different sample concentrations can be eventually obtained in output channels (A_1 – A_7). Figure 6 illustrates the schematic representation of this network. The comparison between experimental data and system simulation results are shown in Table 1, with an average error of 3.6%.

4 CONCLUSION

A composable system simulation framework for complex electrokinetic passive micromixer has been presented, in which an analytical behavioral model library using the analog hardware description language (Verilog-A) has been developed. Kirchhoff’s law and directional signal flow have been employed to solve the electric and concentration networks respectively. The system simulation results have been verified by numerical and experimental data. The proposed interface parameters and behavioral models are able to accurately capture overall effects of system topology, element dimensions, material properties and operational parameters (e.g., electric field) on the mixing performance. Compared with numerical methods, a tremendous speedup (100–10,000×) can be achieved by the composable simulation, while still maintaining high accuracy (relative error less than 5%). Therefore, the framework represents an efficient and accurate simulation tool for system-level synthesis and optimal designs of electrokinetic passive micromixers. While focusing on EK micromixers, the concept of this composable simulation approach can be readily extended to pressure-driven mixers and laminar-diffusion based devices[9, 10].

ACKNOWLEDGEMENT

This research is sponsored by the DARPA and the Air Force Research Laboratory, Air Force Material Command, USAF, under grant number F30602-01-2-0587, and the NSF ITR program under award number CCR-0325344.

REFERENCES

- [1] S. C. Jacobson, T. E. McKnight, J. M. Ramsey, *Analytical Chemistry*, 71, 4455, 1999
- [2] F. Schonfeld, K. S. Drese, S. Hardt, *et al.* MSM’04, 378, 2004.
- [3] Y. Wang, Q. Lin, T. Mukherjee *MicroTAS’04*, 596, 2004.
- [4] Y. Wang, Q. Lin, T. Mukherjee *MSM’04*, 59, 2004.
- [5] <http://www.cadence.com>.
- [6] Y. Wang, Q. Lin, T. Mukherjee, Submitted to *Lab on a Chip*, 2005
- [7] P. Lob, K. S. Drese, V. Hessel, *et al.*, *Chemical Engineering & Technology*, 27, 340-345, 2004
- [8] S. Hardt, F. Schonfeld, *AIChE Journal*, 49, 578-584, 2003
- [9] N. L. Jeon, S. K. W. Dertinger, D. T. Chiu, *et al.*, *Langmuir*, 16, 8311-8316, 2000
- [10] J. P. Brody, P. Yager, *Sensors and Actuators a-Physical*, 58, 13-18, 1997